Supporting Information

Air-Stable n-Type Single-Walled Carbon Nanotubes Doped with Benzimidazole Derivatives for Thermoelectric Conversion and their Air-stable Mechanism

Yuki Nakashima,[†] *Ryohei Yamaguchi,*[†] *Fumiyuki Toshimitsu,*[†] *Masamichi Matsumoto,*[†] *Angana Borah,*[†] *Aleksandar Staykov,*[‡] *Md. Saidul Islam,*[‖] *Shinya Hayami,*[‖] *and Tsuyohiko Fujigaya*[*,†,‡,§,⊥]

[†]Department of Applied Chemistry, Graduate School of Engineering, Kyushu University, 744 Motooka, Nishi-ku, Fukuoka 819-0395, Japan.

[‡]International Institute for Carbon Neutral Energy Research (WPI-I2CNER), Kyushu University, Fukuoka 819-0395, Japan

[§]Japan Science and Technology Agency (JST)-PRESTO, 4-1-8 Honcho, Kawaguchi, Saitama, 332-0012, Japan

[‖] Department of Chemistry, Faculty of Advanced Science and Technology, Kumamoto University, 2-39-1 Kurokami, Chuo-ku, Kumamoto 860-8555, Japan

[⊥] Center for Molecular Systems (CMS), Kyushu University, 744 Motooka, Nishi-ku, Fukuoka 819-0395, Japan.

E-mail address for corresponding author: fujigaya.tsuyohiko.948@m.kyushu-u.ac.jp

Method

Materials: The SWCNTs (Meijo-eDIPS), with a diameter of 1.5 ± 0.5 nm, were purchased from Meijo Nano Carbon. Methanol and acetone were purchased from Kanto Chemical. Ethanol, *N*-methylpyrrolidone (NMP), phosphorus (V) oxide, polyphosphoric acid, tetrahydrofuran (super dehydrated, stabilizer free), and sodium hydride were purchased from Wako Pure Chemical. 1,2-Phenylenediamine (99.5%), salicylic acid, 2-methoxybenzoic acid 4-(1,3-dimethyl-2,3-dihydro-1*H*-benzo[*d*]imidazol-2-yl)-*N*,*N*-dimethylaniline (*N*-DMBI), 1,3-dimethyl-2-(3-nitrophenyl)-2,3-dihydro-1*H*-benzimidazole (*m*-NO_2-DMBI), 2-(2,5-dimethoxyphenyl)-1,3-dimethyl-2,3-dihydro-1*H*-benzimidazole (1,4-MeO-DMBI), 2-(1,3-dimethyl-2,3-dihydro-1*H*-benzo[*d*]imidazol-2-yl)-benzene-1,4-diol (1,4-OH-DMBI), 4-(1,3-dimethyl-2,3-dihydro-1*H*-benzo[*d*]imidazol-2-yl)-2-methoxyphenol (2,3-MeO,OH-DMBI), 2-(1,3-dimethyl-2,3-dihydro-1*H*-benzo[*d*]imidazol-2-yl)-phenol (*o*-OH-DMBI), 4-bromo-2-(1,3-dimethyl-2,3-dihydro-1*H*-benzo[*d*]imidazol-2-yl)-phenol (1,4-OH,Br-DMBI) and 2-(4-fluorophenyl)-1,3-dimethyl-2,3-dihydro-1*H*-benzo[*d*]imidazole (1,3-Cl-DMBI) were purchased from Sigma-Aldrich. Iodomethane and potassium hydroxide were purchased from Tokyo Chemical Industry and Kishida Chemical., respectively.

Preparation of 2-(2-Methoxyphenyl)-1-methyl-1H-benzimidazole: *o*-Phenylenediamime (4.06 g, 37.5 mmol) was added to a salicylic acid (4.56 g, 30 mmol)

solution in poly phosphoric acid (150 mL) and stirred for 5 h at 150 °C. The obtained solution was precipitated in water and $NaHCO_3$ was added to neutralize the solution. The produced solid was collected by vacuum filtration and the washing process was repeated twice. The obtained white solid was dried with phosphoric (V) acid under vacuum at 60 °C. The yield was 68%. ^{1}H NMR (300 MHz, Methanol-d_4, δ) 8.34 (d, J = 7.8 Hz, 1H), 7.65 (dd, J = 3.2 Hz, 2H), 7.49 (t, J = 7.7, 1H), 7.21 (m, J = 3.2 Hz 4H), 7.13 (t, J = 7.7 Hz 1H), 4.03 (s, 3H).

Preparation of 2-(2-Methoxyphenyl)-1,3-dimethyl-1H-benzoimidazol-3-ium iodide (o-MeO-DMBI-I)[S1]: 2-(2-Methoxyphenyl)-1-methyl-1H-benzimidazole (5.0 g, 22.3 mmol) and KOH (13.2 g, 200 mmol) were dissolved in methanol (50 mL) at room temperature under N2 atmosphere. The resulting red solution was treated with methyl iodide (200 mL, 321.3 mmol). The solid appeared and the color of the solution changed to yellow. The reaction was kept at 45 °C for 18 h and was quenched with methanol. The solvent was removed by evaporation. The obtained solid was dissolved in chloroform. The precipitate was removed by filtration and the filtrate thus obtained was evaporated to give a yellow solid. The obtained solid (o-MeO-DMBI-I) was recrystallized from ethanol. The yield was 85%. 1H NMR (300 MHz, Methanol-d_4, δ) 8.01 (dd, J = 3.1 Hz, 2H), 7.86 (t, J = 8.1 Hz, 1H), 7.77 (dd, J = 3.1Hz, 2H), 7.12 (dd, J = 7.65Hz, 1.6 Hz, 1H), 7.44 (d, J = 8.6 Hz,

1H), 7.34 (t, J = 7.65 Hz 1H), 3.94 (s, 3H), 3.92 (s, 6H). Anal. Calcd. For C16H17IN2O, C, 50.54; H, 4.51; I, 33.38; N, 7.37; O, 4.21. Found: C, 50.43; H, 4.51; N,7.36.

Preparation of 2-(2-methoxyphenyl)-1,3-dimethyl-2,3-dihydro-1H-benzimidazole (o-MeO-DMBI)[S2]: $NaBH_4$ (0.28 g, 10.5 mmol) was added to a methanol solution (30 mL) of o-MeO-DMBI-I (2.0 g, 5.26 mmol) in an ice bath. After stirring for 1 hour, the reaction was quenched with methanol and the solid was collected by vacuum filtration. The obtained solid (o-MeO-DMBI) was recrystallized from methanol and a colorless crystal was obtained after drying in vacuum. The yield was 0.63 g (48%). 1H NMR (300 MHz, Methanol-d_4, δ) 7.74 (dd, J = 7.6Hz, 1.7 Hz, 1H), 7.34 (t, J = 7.8 Hz 1H), 7.02, 7.05 (dd, J = 8.3 Hz, 7.6 Hz 2H), 6.41 (dd, J = 2.2Hz, 3.2 Hz, 2H), 6.64 (dd, J = 2.2 Hz, 3.2 Hz, 2H), 3.85 (s, 3H), 2.52 (s, 6H). Anal. Calcd. For C16H18N2O; C, 75.56; H, 7.13; N, 11.01; O, 6.29. Found; C, 75.50; H, 7.09; N, 11.02.

Fabrication of SWCNT Sheets and Doping: The SWCNT sheets were fabricated according to the published procedure.[S3] The thickness of the SWCNT sheet was 30–50 μm. After the SWCNT sheets were cut into 30 mm × 4 mm pieces, the sheets were dipped into 2 mL of an ethanol solution of *o*-MeO-DMBI for 10 min. Solutions of 0.01, 0.1, 1.0, 3.0, 10.0, and 50.0 mM were used. The doped SWCNT

sheets (DMBI-doped SWCNT sheets) were dried in vacuum at room temperature for 12 h.

Measurements: The ^{1}H NMR measurements were carried out using an AV300 M spectrometer (Bruker Biospin). UV–vis–NIR spectra were obtained using V-670 (JASCO). X-ray photoelectron spectroscopy (XPS) was performed using an AXIS-ULTRA (Shimadzu), in which indium was used as the substrate. Au film was measured with each samples and Au $4f_{7/2}$ 84.140 eV was used as the internal standard. The peaks were deconvoluted and the binding energy of C=C bond was used. The thermogravimetric analysis (TGA) was carried out using a TG/DTA 6300 module (SII Nanotechnology) at a heating rate of 10 K min^{-1} under flowing air (100 mL min^{-1}). Scanning electron microscopy (SEM) was carried out using an SU-9000 microscope (Hitachi High Technologies, 10-kV acceleration voltage). The in-plane electrical conductivity and Seebeck coefficient of the samples were determined using a ZEM-3M system (ULVAC-Riko) under helium at a reduced pressure (0.01 MPa). The electrical conductivity and Seebeck coefficient were measured three times at least with different specimens and error range were ±3% and ±1%, respectively. Differential scanning calorimetry (DSC) was carried out using an EXSTAR DSC 6220 calorimeter (SII Nanotechnology) at a heating rate of 10 K min^{-1} under flowing nitrogen (100 mL min^{-1}). Calibration of the specific heat capacity (C_p) was performed using a sapphire crystal (Al_2O_3). The in-plane

thermal diffusivity measured using a Thermowave Analyzer TA (Bethel). The density of the sheets were determined from the weight and volume of the sheets. Thermal conductivity κ was evaluated as $\kappa=C_p \cdot \alpha \cdot \rho$. Time-of-flight mass spectrometry (TOF-MS) was performed using an Autoflex III system (BRUKER) using *o*-MeO-DMBI-doped SWCNT sheets. The surface area of *o*-MeO-DMBI was calculated using the Maestro interface (Schrödinger, LLC). Gas adsorption (77 K, $1 \times 10^{-8} < P/P^0 < 1$) measurements were conducted using the BELSORP-mini instrument (BEL Japan, Inc.) after pretreatment at 300 °C for 12 hours under high vacuum.

Adsorption Isotherm Measurements: SWCNT sheet was dipped in ethanol solution of *o*-MeO-DMBI (2.0 mL) with different concentration at 25 ºC. After standing for 50 hour, the SWCNT sheet was taken out and UV-vis spectra was measured. Concentration of *o*-MeO-DMBI cation in the solution together with the *o*-MeO-DMBI adsorbed onto the SWCNT sheet were calculated based on the calibration curve of *o*-MeO-DMBI-I.

Molecular Modeling: Structural simulation was carried out based on molecular mechanics (MM) calculation by MacroModel program (Schrodinger, version 10.2) using OPLS 2005 as the force fields.[S4]

Theoretical Calculations: Periodic, plane-wave DFT calculations and first-principles molecular dynamics were performed with the Vienna Ab initio Software Package (VASP).[S5-8] The Perdew–Burke–Ernzerhof (PBE) exchange-correlation functional was applied using projector augmented-wave pseudopotentials. Electron energies were converged to 10^{-5} eV using Gaussian smearing. The calculations were performed with a 433-eV cut-off energy and Gamma k-points sampling. The tubes were placed in periodic boxes with dimensions of 2.0 nm × 2.0 nm × 1.5 nm. Geometry optimization was performed using the conjugated gradient algorithm. Relaxation was performed for the atomic positions only. The relaxation was performed until the forces converged to values below 0.03 eV $Å^{-2}$. Binding energies were calculated as the difference in energy of the CNT-molecule system and the energies of the tube and molecule separately.[S9] The electron density difference map was estimated in a similar way. This was obtained as the difference between the electron density of the CNT-molecule system and the electron density energies of the tube and molecule separately. Spin density plots were obtained as the difference in the majority spin and minority spin electron densities. Charges were determined using Bader population analysis.[S10] We investigated (6,6) SWCNT as the model SWCNT. Throughout the theoretical calculations, the graphical visualization package VESTA was used.[S11]

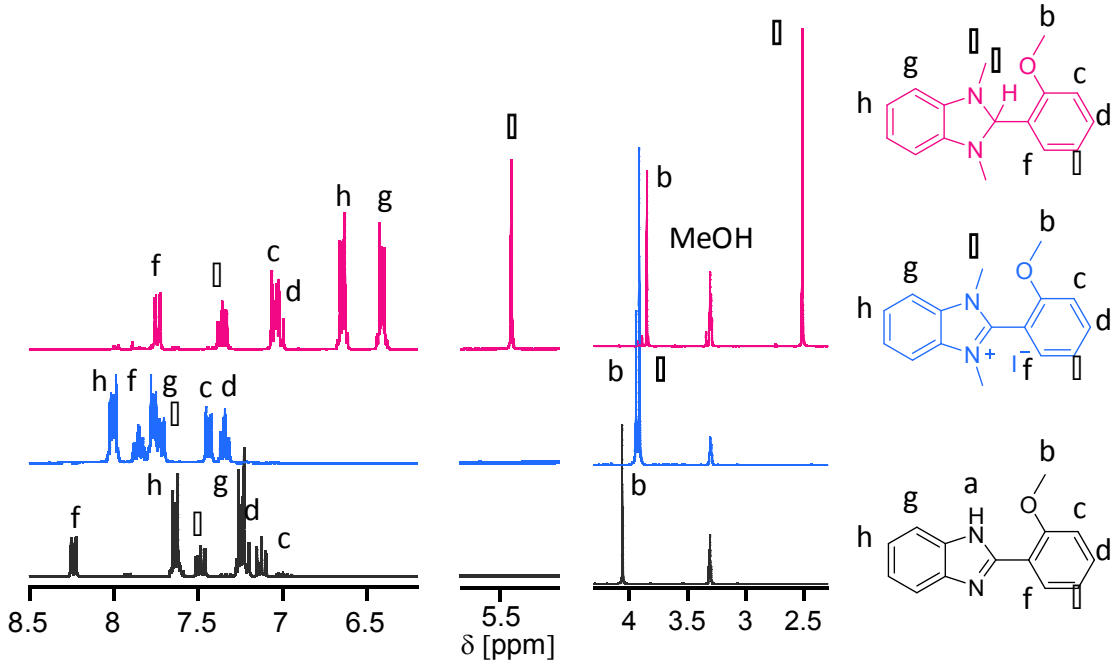

Figure S1. ^{1}H-NMR of 2-(2-Methoxyphenyl)-1-methyl-1H-benzimidazole (black), *o*-MeO-DMBI-I (blue) and *o*-MeO-DMBI (red) measured in Methanol-d_4.

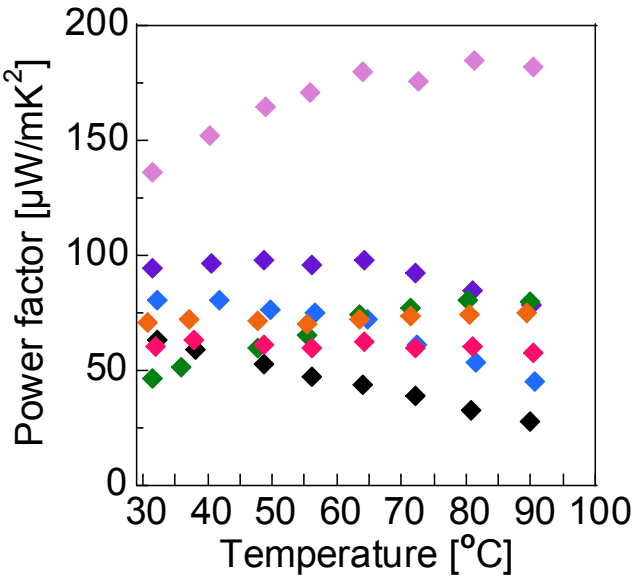

Figure S2. Temperature dependence of power factor of the SWCNT sheets doped with 0 (black), 0.01 (blue), 0.10 (purple), 1.0 (green), 3 (pink), 10 (orange) and 50 mM (red) of *o*-MeO-DMBI solutions.

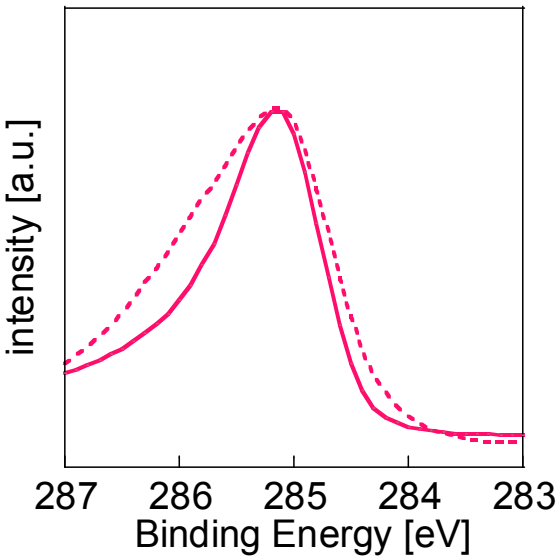

Figure S3. C1s core level peaks of SWCNT sheets doped with 10.0 mM *o*-MeO-DMBI solutions before (solid line) and after 160 days (dotted line) cumulated air exposure.

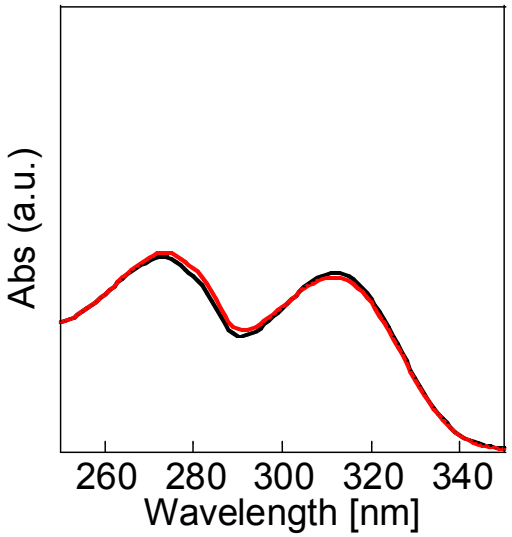

Figure S4. UV-vis absorption spectra of *o*-MeO-DMBI solutions in ethanol after 0 (black line) and 50 hours (red line).

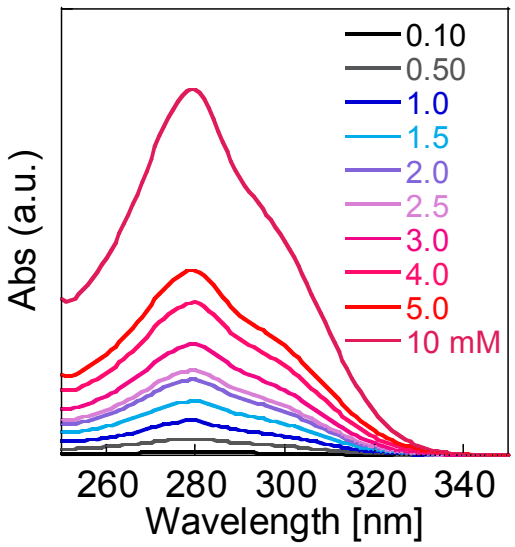

Figure S5. UV-vis absorption spectra of *o*-MeO-DMBI-I solutions in ethanol at various concentration.

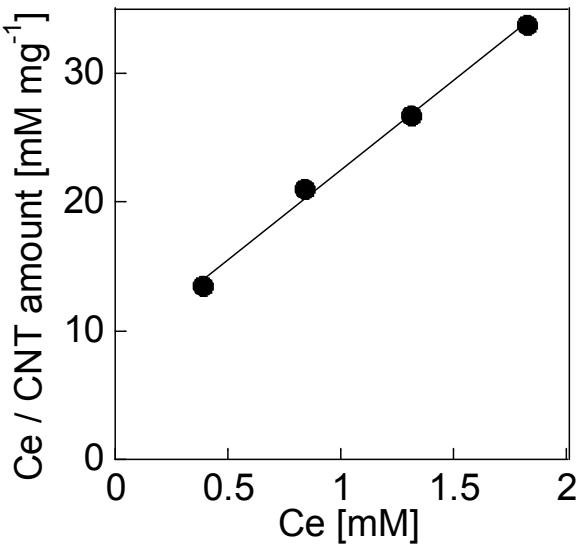

Figure S6. Langmuir adsorption isotherm of *o*-MeO-DMBI onto SWCNT sheets, where Ce is equilibrium concentration.

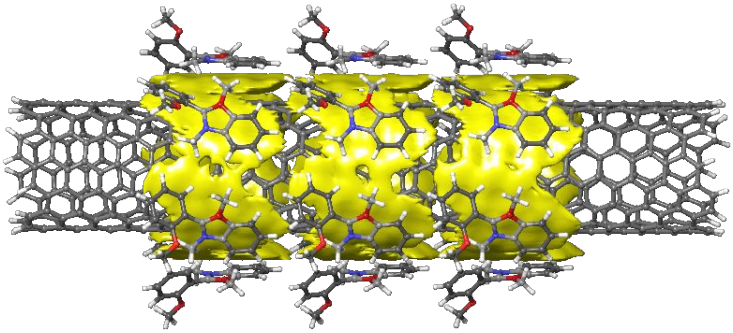

Figure S7. Optimized monolayer structure of the 18 *o*-MeO-DMBI molecules on (8,6)SWCNT. 18 *o*-MeO-DMBI were found to cover 830 Å^2.

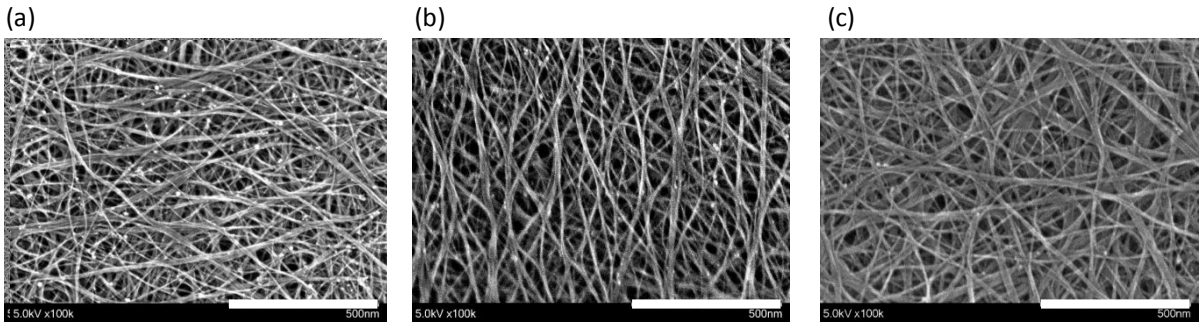

Figure S8. SEM images of (a) non-doped, (b) 10.0 mM and (c) 50 mM-doped SWCNT sheets. Scale bars: 500 nm.

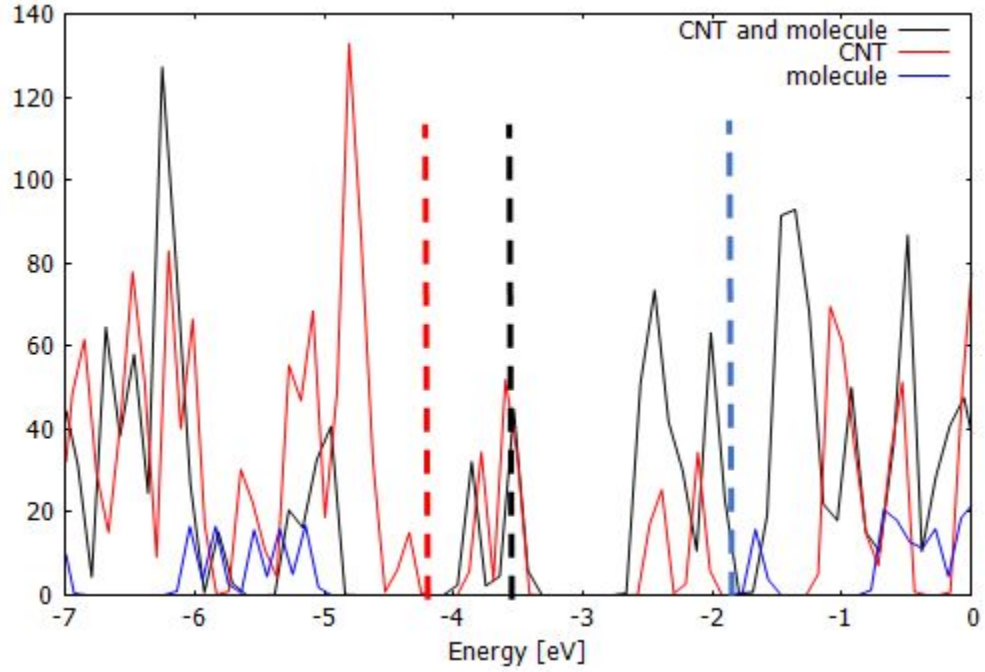

Figure S9. Aligned DOS plots for SWCNT-*o*-MeO-DMBI complex (black line), SWCNT (red line), and *o*-MeO-DMBI (blue line). Fermi energies are denoted with dashed lines. The DOS maps are aligned to the vacuum level (0.0eV).

Supporting Information References

(S1) Wei, P.; Menke, T.; Naab, B. D.; Leo, K.; Riede, M.; Bao, Z. 2-(2-Methoxyphenyl)-1,3-Dimethyl-1h-Benzoimidazol-3-Ium Iodide as a New Air-Stable N-Type Dopant for Vacuum-Processed Organic Semiconductor Thin Films. *J. Am. Chem. Soc.* **2012**, *134*, 3999-4002.

(S2) Wei, P.; Liu, N.; Lee, H. R.; Adijanto, E.; Ci, L.; Naab, B. D.; Zhong, J. Q.; Park, J.; Chen, W.; Cui, Y.; Bao, Z. Tuning the Dirac Point in Cvd-Grown Graphene through Solution Processed N-Type Doping with 2-(2-Methoxyphenyl)-1,3-Dimethyl-2,3-Dihydro-1h-Benzoimidazole. *Nano Lett.* **2013**, *13*, 1890-1897.

(S3) Nakashima, Y.; Nakashima, N.; Fujigaya, T. Development of Air-Stable N-Type Single-Walled Carbon Nanotubes by Doping with 2-(2-Methoxyphenyl)-1,3-Dimethyl-2,3-Dihydro-1h-Benzo[D]Imidazole and Their Thermoelectric Properties. *Synth. Met.* **2017**, *225*, 76-80.

(S4) Mohamadi, F.; Richards, N. G. J.; Guida, W. C.; Liskamp, R.; Lipton, M.;

Caufield, C.; Chang, G.; Hendrickson, T.; Still, W. C. Macromodel—an Integrated Software System for Modeling Organic and Bioorganic Molecules Using Molecular Mechanics. *J. Comput. Chem.* **1990**, *11*, 440-467.
(S5) Kresse, G.; Furthmüller, J. Efficiency of Ab-Initio Total Energy Calculations for Metals and Semiconductors Using a Plane-Wave Basis Set. *Comput. Mater. Sci.* **1996**, *6*, 15-50.
(S6) Kresse, G.; Furthmüller, J. Efficient Iterative Schemes for Ab Initio Total-Energy Calculations Using a Plane-Wave Basis Set. *Phys. Rev. B* **1996**, *54*, 11169-11186.
(S7) Blöchl, P. E. Projector Augmented-Wave Method. *Phys. Rev. B* **1994**, *50*, 17953-17979.
(S8) Kresse, G.; Hafner, J. Ab Initio Molecular Dynamics for Liquid Metals. *Phys. Rev. B* **1993**, *47*, 558-561.
(S9) Staykov, A.; Ooishi, Y.; Ishihara, T. Immobilizing Metal Nanoparticles on Single Wall Nanotubes. Effect of Surface Curvature. *J. Phys. Chem. C* **2014**, *118*, 8907-8916.
(S10) Tang, W.; Sanville, E.; Henkelman, G. A Grid-Based Bader Analysis Algorithm without Lattice Bias. *J. Phys.: Condens. Matter* **2009**, *21*, 084204.
(S11) Momma, K.; Izumi, F. Vesta 3 for Three-Dimensional Visualization of Crystal, Volumetric and Morphology Data. *J. Appl. Crystallogr.* **2011**, *44*, 1272-1276.